Integrated Compensation-based Laser Sensor System for In-plane and Out-of-plane Target Tracking

ERNST CSENCSICS[1,*]

[1] *Automation and Control Institute, Vienna University of Technology, Vienna, Austria*
[*] *csencsics@acin.tuwien.ac.at*

Abstract:
This paper presents the development of a compensation-based laser sensor system, capable of sensing in-plane as well as out-of-plane displacements of a target. The sensor design integrates principles of laser triangulation and objective laser speckle measurement into a single device and provides an in-plane and out-of-plane resolution of 3 μm and 1 μm, respectively. The compensation-based operation keeps the variation of distance and lateral position relative to the target close to zero by actively following the target motion using feedback control. This enables a large operation range of the resulting sensing and tracking system, limited only by the range of the actuation system. Accurate tracking of target motions is demonstrated in an area of 1 x 1 mm with a small remaining spatial rms tracking error between 8.75 μm and 13.25 μm.

1. Introduction

Applications in which the surface of a target, object or product piece needs to be tracked by a manipulating or measuring tool in order to enable high precision processing or measurements are commonly encountered. They range from industry and manufacturing [1,2] all the way to medicine and life sciences [3,4]. A particular application case, which is of highest interest for the manufacturing industry, are flexible high precision 3D measurements on free formed surfaces directly in the production line [5]. To enable high throughput and compensate for vibrations of the production environment during the measurement process, these systems are desired to actively track the motion of a moving target for maintaining a constant position of the inspection tool relative to the target [1,6]. Figure 1 shows such a system concept with a feedback controlled robot carrying a platform with a scanning inspection tool [7] and a tracking sensor (TS), which measures the distance and lateral position to the target and is preferably based on non-contacting optical principles to minimize physical interaction.

For measuring out-of-plane displacements there are plenty of optical principles with compact sensor heads available, such as laser triangulation, chromatic confocal sensors, or interferometers [8]. Due to their robustness, large measurement range and high resolution, laser triangulation sensors are one of the most commonly used sensors in dimensional measurement and quality control in industry [9]. In contrast, optical measurement principles for measuring in-plane displacement, enabling compact sensor devices, are hardly available. One example are digital image correlation methods, which for the classical case of white light illumination, however, require a target surface with macroscopic features or the unfavorable use of markers [10].

Laser speckle based measurement principles have recently been introduced for this purpose, offering advantages such as high resolution, contact-less measurements and applicability to most technical surfaces without the need for additional markers [11]. Apart from electronic speckle pattern interferometry [12], which requires a quite complex sensor structure, particularly measurement assemblies based on objective laser speckles (OLSPs), which do not suffer from lens aberrations and have high potential for miniaturization, are of interest [13]. They are, however, suffering from translational speckle pattern decorrelation, which rapidly increases measurement

Post-print version of the article: E. Csencsics, "Integrated Compensation-based Laser Sensor System for In-plane and Out-of-plane Target Tracking," *Applied Optics*, vol. 59, no. 20, p. 6138-6147, 2020. DOI: 10.1364/AO.395572

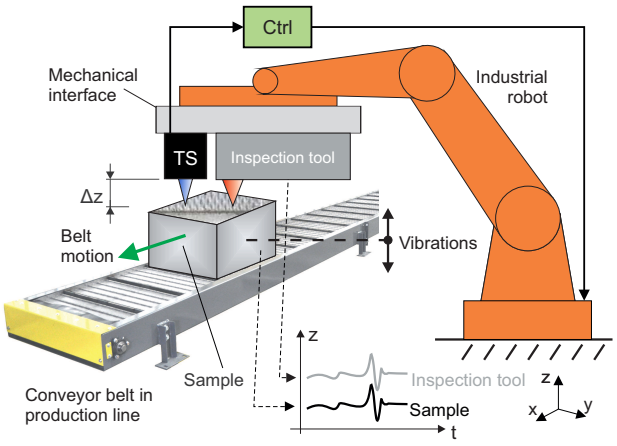

Fig. 1. Tracking a moving target sample in an industrial production line. A robot carries the scanning inspection tool, conducting precision measurements on the sample surface. The tracking sensor (TS) detects displacements of the sample and enables tracking of the sample motion in-plane (conveyor motion) and out-of-plane (vibrations) via the feedback controlled robot.

uncertainty and limits their operation range to below the laser spot diameter [14]. For this reason OLSP assemblies have mainly been used for strain measurement in the past [15,16]. Recently they have also been applied for tool speed measurements [17] as well as for integration-based relative position sensing [18], which overcomes the limitation by re-setting the reference image for larger displacements. This, however, leads to the accumulation of measurement errors, which limits the accuracy with increasing range of motion. They have also been implemented for absolute position sensing on a steel rod together with a feature-based probabilistic framework [19].

A promising approach to overcome the limited operation range for the application of tracking a target is the advancement to a compensation-based OLSP displacement measurement [14]. The compensation-based approach holds the speckle pattern displacement close to zero, thus compensating the translational pattern decorrelation, by actively tracking the illuminated area using external actuation and feedback control. This exactly resembles the targeted application case (see Fig. 1). With the sensing system turned into a zero detector, the feedback controller output is a direct measure for the displacement, which is a well known technique e.g. in atomic force microscopy [20]. This enhances the operation range of the measurement system essentially to the range of the positioning system, e.g. the robot.

In order to obtain a single integrated sensor for all linear degrees of freedom (DoF), the OLSP assembly is extended by an aperture, which reduces the illuminated detector area and introduces an additional triangulation geometry, enabling the simultaneous measurement of out-of-plane motions. The contribution of this paper is the design and analysis of the integrated compensation-based laser sensor system, which enables simultaneous measurement of linear in-plane and out-of-plane displacements of a target with an optically rough surface. It integrates the properties of objective laser speckle measurement [13] and laser triangulation sensing [21] and is combined with actuators and feedback control to track the motion of a target in the out-of-plane and one in-plane DOF. The sensor design has a simple structure and reduces the number of required components, enabling a compact and light sensor head with potential for miniaturization for the purpose of system integration. With the two utilized measurement principles discussed in Section 2, the integrated laser sensor is designed in Section 3. In Section 4 an experimental sensor

Post-print version of the article: E. Csencsics, "Integrated Compensation-based Laser Sensor System for In-plane and Out-of-plane Target Tracking," *Applied Optics*, vol. 59, no. 20, p. 6138-6147, 2020. DOI: 10.1364/AO.395572

setup is developed and a suitable control structure for implementing the compensation-based measurement principle is designed. Section 5 shows the results of tracking experiments for motion in single DoFs and combined motions of the target, while Section 6 concludes the paper.

2. Measurement Principles

To measure in-plane as well as out-of-plane motions of a target, in order to compensate for them, the integrated laser sensor combines principles of laser triangulation sensing and objective laser speckles measurement.

2.1. Laser Triangulation Sensing

In laser triangulation sensors a laser beam is directed towards a target object and the light scattered at the spot where the beam hits the target is used to observe the point of intersection. The scattering behavior of the target surface depends on its texture and structure as well as on the wavelength of the illuminating laser. Under a certain angle, with respect to the direction of the incident laser beam, the light spot on the target is imaged onto a position sensitive detector (PSD) via an objective [21]. The position of the spot image on the detector depends on the location of the laser spot and thus the position of the target in z-direction. With the obtained position on the detector, the incident direction and the known sensor geometry, the distance of the target in z-direction can be determined [8], [22]. Figure 2a shows a schematic of the most common laser triangulation sensor assembly, measuring out-of-plane motion of a target, with Θ the triangulation angle in the center of the measurement range. It is apparent that specular reflecting surfaces are in general not suited for measurements with the shown assembly but require specific system designs with tilted laser source and tilted detector [23].

The components of a triangulation sensor are typically assembled according to the Scheimpflug condition in order to obtain a sharp spot image on the detector independent of the target distance [24]. The sensor characteristic, which is the relation of the displacement of the target to the displacement of the imaged spot on the detector, is in general non-linear, which means that the sensitivity of the sensor is non-constant. This is caused by the relative geometrical tilt of the components with respect to each other and can be calculated analytically [21]. To determine the spot location on the detector, the center of gravity (CoG) of the projected light spot is calculated. Besides the beam propagation and profile, the target surface properties and the imaging aberrations, the accuracy of the CoG calculation is mainly influenced by laser speckles on the imaging detector [8]. The speckles represent a limit on the achievable accuracy and resolution of the sensor, being considered undesired effects of the coherent illumination and have been studied in this relation in the past [25].

2.2. Objective Laser Speckle Measurement

When an optically rough surface is illuminated by coherent light, each spot on the micro-structured surface is considered as individual scatterer, scattering the incoming light randomly in direction, amplitude and phase. The scattered waves propagate away from the surface while interfering with each other. When this interference effect is imaged as a spatial intensity distribution in the diffraction field or with an objective, a grainy pattern of bright and dark spots, termed laser speckle pattern, is obtained [26].

When using a focused lens system, as with a typical laser triangulation sensor, subjective laser speckles (SLSPs) can be observed. In this case, the aperture limits the spatial interaction of the individual waves emerging from the surface [27]. Objective Laser Speckle Patterns are observed when no imaging system is used (free space observation), such that the entire illuminated area contributes to the resulting speckle pattern. Focusing on the lens-less case with OLSPs for reasons of compactness and the absence of lens aberrations [13], Fig. 2b shows the configuration of an OLSP sensor for measuring in-plane displacements along the x- and y-axis. The optically

Post-print version of the article: E. Csencsics, "Integrated Compensation-based Laser Sensor System for In-plane and Out-of-plane Target Tracking," *Applied Optics*, vol. 59, no. 20, p. 6138-6147, 2020. DOI: 10.1364/AO.395572

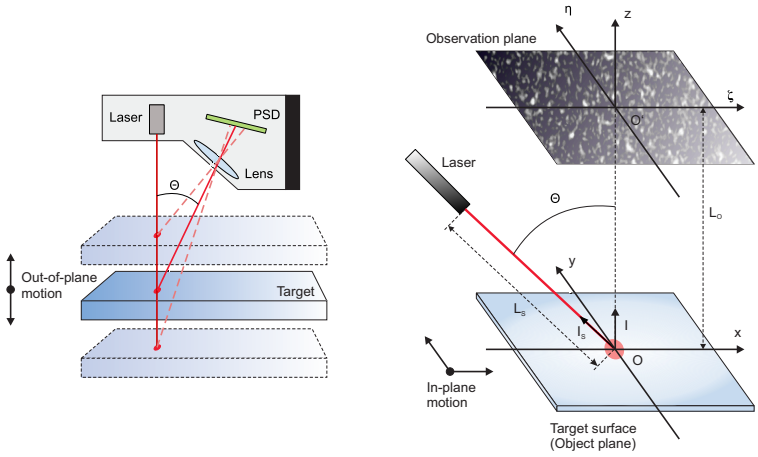

(a) Laser triangulation sensor. (b) Objective laser speckle assembly.

Fig. 2. Laser triangulation sensor principle and objective speckle measurement. (a) depicts the working principle of a triangulation sensor, which is based on the displaced spot on the position sensitive detector (PSD) and precise geometric relations. (b) shows the assembly of an objective laser speckle sensor with laser source object and detector.

rough target surface is illuminated by a laser in the xz-plane, which is a distance L_S away from the origin O and tilted by an angle Θ with respect to the surface normal. The image sensor is placed in the observation plane, which is parallel to the object plane (without loss of generality) and located at the distance L_O. Neglecting rotations and stress, the displacement of the speckle pattern in ζ(x)- and η(y)-direction caused by a displacement of the target can be expressed by [13]

$$A_\zeta = -a_x \left[\frac{L_O}{L_S}(l_{Sx}^2 - 1) + l_x^2 - 1\right] - a_y \left[\frac{L_O}{L_S} l_{Sx} l_{Sy} + l_x l_y\right] - a_z \left[\frac{L_O}{L_S} l_{Sx} l_{Sz} + l_x l_z\right], \quad (1)$$

$$A_\eta = -a_x \left[\frac{L_O}{L_S} l_{Sx} l_{Sy} + l_x l_y\right] - a_y \left[\frac{L_O}{L_S}(l_{Sy}^2 - 1) + l_y^2 - 1\right] - a_z \left[\frac{L_O}{L_S} l_{Sy} l_{Sz} + l_y l_z\right] \quad (2)$$

with $a_{x,y,z}$ the displacements of the target in the three translational DoFs. For the nominal case of a parallel object and observation plane the simplified unit vectors $\vec{l} = (l_x, l_y, l_z)^T = (0,0,1)^T$ and $\vec{l_S} = (l_{Sx}, l_{Sy}, l_{Sz})^T = (sin(\Theta), 0, cos(\Theta))^T$ given in Fig. 2b are obtained. If the two planes are not parallel, also small crosstalk terms may need to be considered.

For the given assembly the pattern displacement component in η-direction reduces to $A_\eta = a_y(L_O/L_S + 1) = k_y \cdot a_y$, so that there is no crosstalk from out-of-plane displacements and the sensitivity k_y is independent of Θ. For practical applications with large values of L_S the sensitivity k_y will always reside around 1 and can be obtained for a given geometry [14]. The pattern displacement component in ζ-direction reduces to $A_\zeta = a_x \left[1 - L_O/L_S \cdot cos^2(\Theta)\right] - a_z \cdot L_O/2L_S \cdot sin(2\Theta)$, showing a Θ-dependent sensitivity k_x as well as a crosstalk component from out-of-plane motions, which gets diminished for decreasing values of Θ.

To estimate the speckle pattern displacement, the two-dimensional normalized cross-correlation function (NCC) is most commonly applied to the shifted version and a reference image [28].

Post-print version of the article: E. Csencsics, "Integrated Compensation-based Laser Sensor System for In-plane and Out-of-plane Target Tracking," *Applied Optics*, vol. 59, no. 20, p. 6138-6147, 2020. DOI: 10.1364/AO.395572

A direct estimate for the spatial displacement is given by the position of the NCC peak value with a resolution of ±1/2 pixel, without additional interpolation. The use of laser speckles for displacement measurement is always limited by decorrelation effects caused by three major factors: (i) changes in the microstructure due to stress or strain, (ii) the relative overlap of the correlation windows and (iii) changes of the illumination position on the surface due to target displacement. In the case of translational applications without strain, the first factor can be neglected. The influence of the second factor can be decreased by either an increased size of the correlation window or sub-pixel interpolations [29]. The third factor describes the reduced overlapping area of two light spots caused by a displacement of the target, which limits the measurement range to below the diameter of the light spot [14]. This aspect will be revisited in Section 4.2.

3. Compensation-based Integrated Laser Sensor Design

To measure and track in-plane and out-of-plane displacements of a target, the integrated laser sensor design combines the principles of laser triangulation and objective speckle sensing. Starting from the assembly in Fig. 2b, the setup is extended by an aperture which is mounted in a distance L_p parallel to the target and reduces the detector area which is effectively illuminated by the speckle pattern. The aperture is significantly larger than the diameter of the illuminating laser

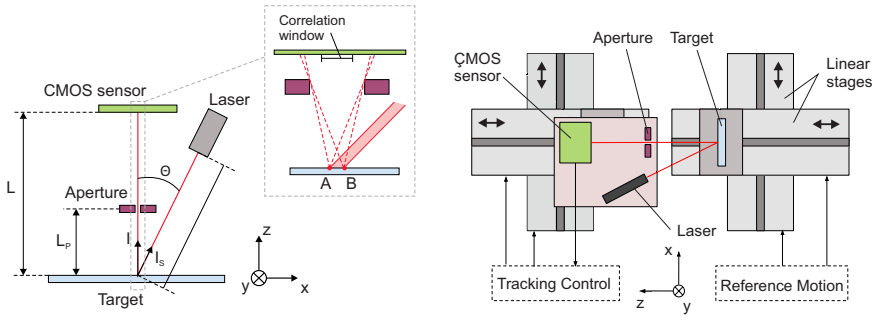

(a) Combined sensor assembly. (b) Schematic of experimental setup.

Fig. 3. Compensation-based sensor setup with aperture integrating the triangulation and the OLSP sensing principle. (a) shows a schematic of the combined sensor assembly. (b) depicts a schematic of the experimental setup with two pairs of positioning stages for in-plane and out-of-plane displacement.

beam, so that the bundle of rays originating from the illuminated surface area is not modified in the detector area around the correlation window and is still forming objective speckles (zoomed image in Fig. 3a). The proposed configuration is equivalent to the triangulation sensor assembly in Fig. 2a when the locations of detector and laser are switched and the lens is replaced by the aperture, which is now parallel to the detector. To measure out-of-plane displacement the shift of the CoG of the illuminated area on the detector can be used, which results from a laterally shifted location of the incident beam on the displaced target. The sensor thus uses the information in the speckle pattern as well as the location of the pattern, i.e. the illuminated area, on the detector. Compared to the initial triangulation sensor design this adapted version has a geometry induced reduced sensitivity to out-of-plane displacements, which is a factor of $cos(\Theta)$ smaller.

In order to obtain a large range tracking system, able to follow the motion of a target, the assembly from Fig. 3a is placed on a tracking platform on a stack of translational stages, as shown in Fig. 3b, which are arranged parallel to the reference stages, displacing the target in x- and

Post-print version of the article: E. Csencsics, "Integrated Compensation-based Laser Sensor System for In-plane and Out-of-plane Target Tracking," *Applied Optics*, vol. 59, no. 20, p. 6138-6147, 2020. DOI: 10.1364/AO.395572

z-direction, and are used to follow the target motion via feedback control. By this approach the integrated laser sensor is turned into a zero detector, which can be used (i) for actively tracking the target and (ii) for compensation-based measurements of the target position by evaluating the controller output of the tracking stage. This significantly reduces the translational decorrelation effect and increases the measurement range of the integrated laser sensor.

The system configuration shown in Fig. 3b, which is used to evaluate the integrated laser sensor for one in-plane and one out-of-plane DoF, implements the OLSP configuration which is sensitive to crosstalk from out-of-plane motion (see (1)), in order to investigate inter-dependencies between the two principles for in-plane and out-of-plane motions. For this case the illuminating laser is placed in the plane generated by the x- and z-axis. By adding two additional linear stages for actuating the target and the tracking platform in y-direction, respectively, the tracking system can be easily extended to all three translational DoFs [14].

4. Experimental Prototype Setup

4.1. Setup Implementation

To evaluate the compensation-based integrated laser sensor, the setup shown in Fig. 4 is developed. It comprises two linear stages to displace the target (Type: VT-80 62309120, Physik Instrumente (PI) GmbH, Germany) and two stages to actuate the tracking platform with the sensor (Type: VT-80 62309140, Physik Instrumente (PI) GmbH, Germany), which all provide internal position sensors with a resolution of 500 nm. The built-in feedback position control enables a uni-

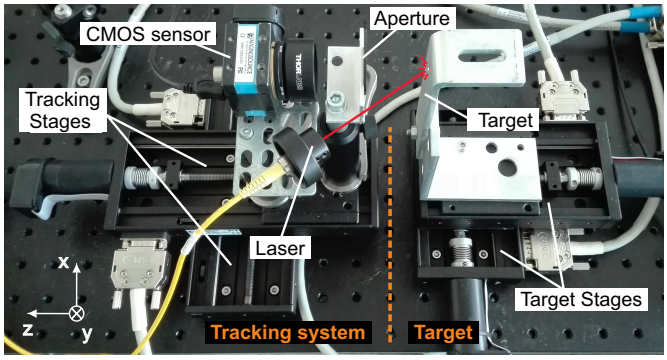

Fig. 4. Experimental tracking prototype setup. The metal target is displaced by two position controlled stages. The integrated laser sensor assembly consisting of laser source, aperture and sensor is placed on two tracking stages, which follow the motion of the target based on the information of the laser sensor.

directional motion precision of 800 nm. The grey scale CMOS camera sensor (Type: DMK 22BUC03, Imaging Source GmbH, Germany) has 744 x 480 pixel, which are 6-by-6 μm in size, a maximum frame rate of 76 fps and is mounted without any focusing optics. The laser source is a linear polarize HeNe laser (Model: 1108P, JDSU, CA, USA) with a wavelength of 632.8 nm and an output power of 0.5 mW. The laser is coupled into a single-mode fiber (yellow cable) and again collimated at the fiber output, resulting in a beam diameter of 430 μm and an output power of 600 μW. The collimated beam is directed towards the target under and angle of $\Theta \approx 30°$. The target is an ordinary aluminium part with raw, non-modified surface. The aperture is formed by an optical alignment target (SCPA1, Thorlabs Inc., NJ, USA) with an aperture diameter of 1 mm.

The image processing is done in MATLAB (MathWorks Inc., MA, USA). The setup is designed to obtain a speckle size of about 10 pixel, which is calculated via auto-correlation to 61 μm

Post-print version of the article: E. Csencsics, "Integrated Compensation-based Laser Sensor System for In-plane and Out-of-plane Target Tracking," *Applied Optics*, vol. 59, no. 20, p. 6138-6147, 2020. DOI: 10.1364/AO.395572

(full-width at half maximum) along the x-axis [30]. To obtain a reasonable tradeoff between required computational effort and decorrelation effects due to a reduced correlation window overlap, the correlation window size is set to 64 x 64 pixel. Together with a two-fold interpolation this leads to a resolution of ±1/4 pixel (3 μm). Due to the limited frame rate of the CMOS camera sensor, the data transfer to and the image processing on an external PC, the sample rate of the sensor system is about 10 Hz.

4.2. Setup Evaluation

For evaluation of the experimental setup the influence of the aperture and its distance to the target is investigated in terms of the resulting speckle field, the sensitivity and crosstalk for in-plane and out-of-plane displacement as well as the static decorrelation curve.

In Fig. 5 the OLSP field on the CMOS sensor is shown for the setup without mounted aperture, as well as for the aperture mounted in distances of 30 mm and 55 mm with respect to the target. The used correlation window size is also depicted in Fig. 5c. The window should still lie within a fully developed OLSP pattern, to obtain meaningful results for in-plane displacements, such that for the chosen aperture significantly larger distances are not applicable. With increasing distance to the target the aperture reduces the effectively illuminated detector area (cf. also Fig. 3a) but also decreases the sensitivity of the integrated laser sensor for out-of-plane motion due to the triangulation-geometry-induced decreasing dislocation of the illuminated area and thus its CoG.

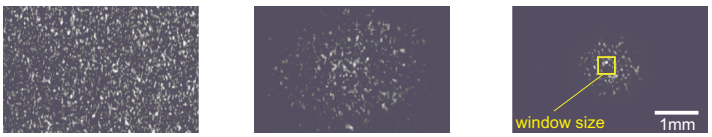

Fig. 5. Speckle field on the detector in dependence of aperture position. (a) shows the OLSP field with no aperture mounted, while (b) depicts the narrowed speckle field for the aperture at distance L_P = 30 mm and (c) for the aperture at L_P = 55 mm. The size of the used correlation window is shown in yellow.

To investigate the sensitivity, the tracking platform with the integrated laser sensor remains static, while the target platform performs single-axis sinusoidal motion in x- and z-direction with an amplitude of 100 μm. Figure 6 shows the sensor outputs for the aperture located at 30 mm and 55 mm. Evaluating the correlation peak shift as measure for in-plane displacement in Fig. 6a, shows that both configurations (solid red and dash-dotted black), as well as the configuration without aperture (data not shown), obtain comparable results. The resulting sensor gain of about $k_x \approx 0.98$ matches the derivations from Section 2.2. The crosstalk from in-plane motion to the shift of the CoG is small for both configurations (solid green and dashed black) with the peak-to-valley value remaining below one pixel size. Evaluation of the CoG shift as measure for out-of-plane displacement in Fig. 6b, shows that the sensitivity clearly increases for smaller distances L_P of the aperture to the target and that it is smaller than for in-plane motion, which is due to the different measurement principles. The sensitivity is non-constant, as expected from literature [21], and increases for target motions towards the sensor system. However, around zero displacement, which is the eventual range of operation, the system with the aperture at 55 mm results in a low sensitivity of 0.09 μm/μm (dashed black), while placing the aperture at 30 mm increases the sensitivity to 0.72 μm/μm (solid green). The crosstalk is slightly higher for the configuration with the aperture at 30 mm. However, as the integrated laser sensor will only be used as zero detector, again mainly the region around zero displacement is of interest. For displacements of ±26 μm around zero there is no shift of the correlation peak observable (solid

Post-print version of the article: E. Csencsics, "Integrated Compensation-based Laser Sensor System for In-plane and Out-of-plane Target Tracking," *Applied Optics*, vol. 59, no. 20, p. 6138-6147, 2020. DOI: 10.1364/AO.395572

red and dash-dotted black), such that the crosstalk in this motion range can be neglected.

In order to obtain a high sensitivity but still reduce the effectively illuminated detector area at the same time (see Fig. 5b), the aperture is placed at L_p = 30 mm. The resolution of the resulting configuration is 3 μm in x-direction, determined by half a pixel size due to the two-fold interpolation, and 1 μm in z-direction, which is given by the smallest position step that can still be resolved (data not shown).

The measured static decorrelation curves of the setup with no aperture (dotted blue) and with the aperture at 30 mm (dotted grey) are depicted in Fig. 7. As the translational decorrelation can be modeled geometrically by the reduced overlap area of two circular spots with Gaussian intensity distribution caused by a displacement of the surface, the simulation result for an assembly without aperture and a $1/e^2$ beam diameter of 430 μm is also shown (solid red) [14]. The measurements without aperture show good agreement with the simulation and indicate that already a small spot shift of 20% reduces the pattern correlation value to 0.65. The measurements with aperture lie constantly below those without aperture, which may be explained by alignment

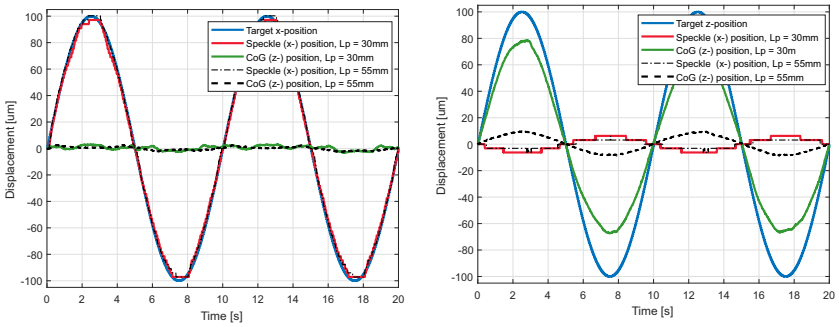

(a) In-plane (x-direction) displacement.

(b) Out-of-plane (z-direction) displacement.

Fig. 6. Sensitivity of speckle correlation peak and CoG shift to in-plane and out-of-plane displacement in dependence of the aperture position L_p (30 mm and 55 mm). (a) shows the sensitivity to displacement in x-direction. (b) shows the sensitivity to displacement in z-direction.

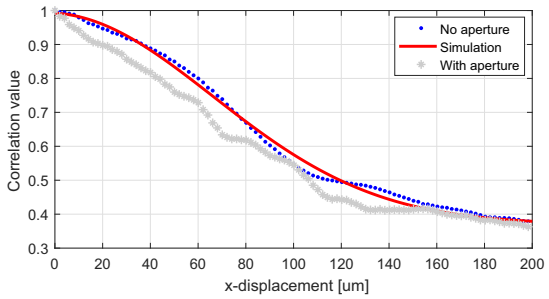

Fig. 7. Speckle pattern decorrelation for in-plane target displacement with and without aperture. The data measured with no aperture (blue dots) shows good agreement with the simulation (red line). The decorrelation slope measured with installed aperture (grey stars) shows a slightly steeper decay than without it.

Post-print version of the article: E. Csencsics, "Integrated Compensation-based Laser Sensor System for In-plane and Out-of-plane Target Tracking," *Applied Optics*, vol. 59, no. 20, p. 6138-6147, 2020. DOI: 10.1364/AO.395572

uncertainties of the spot on the target and the aperture with respect to the detector. The average speckle size with aperture is determined to 57.6 μm (9.6 pixel), indicating that the speckle size is practically not affected by integration of the aperture, as already explained in Section 3.

4.3. Control Design

A schematic block diagram of the feedback control system designed for implementing the compensation-based measurement system is depicted in Fig. 8. The reference signals of the

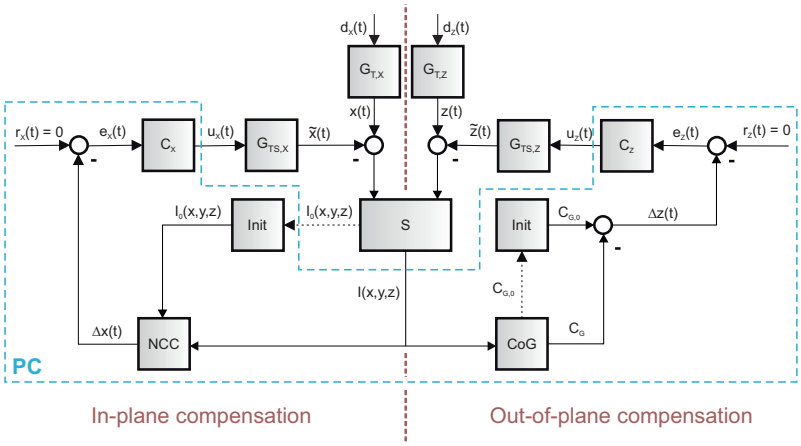

Fig. 8. Block diagram of the tracking control structure. The CMOS sensor samples the OLSP pattern I, which is correlated against a reference pattern I_0 to obtain Δx. The center of gravity of the pattern C_G is calculated and compared against the reference location $C_{G,0}$ to obtain Δz. The two feedback tracking controllers compensate for the displacement by adjusting the setpoints u_X and u_Z of the x- and z-tracking stage, respectively.

target stages d_x and d_z lead to the displacements x and z, which essentially act as disturbances on the system. The CMOS sensor S captures the current speckle pattern I, which is displaced by $x - \tilde{x}$ and compares it to the initial speckle pattern I_0, which is stored as reference image. The measured displacement on the detector Δx is calculated by determining the shift of the NCC peak value. The feedback tracking controller C_X aims to keep the error e_x at zero and compensates for the measured displacement by calculating a new set-point u_x for the x-tracking stage $G_{TS,X}$, in order to follow the motion of the target stage $G_{T,X}$. Similarly, the CoG of the current image C_G is calculated and compared to the CoG of the initially stored reference image $C_{G,0}$, resulting in the shift Δz. The feedback tracking controller C_Z compensates for the out-of-plane displacement by setting a new set-point u_z for the z-tracking stage $G_{TS,Z}$.

The used tracking controllers are integral controllers, which are tuned by increasing the gain until the respective linear stage becomes marginally stable and starts to oscillate and then reducing it by 15%, resulting in I-gains of $K_{i,x} = 0.05$ and $K_{i,z} = 0.04$. It is assumed that the system is operated at speeds well below the bandwidth of the designed tracking controllers, where the dynamics of the internally position controlled target stages $G_{T,X}$ and $G_{T,Z}$ as well as of the tracking stages $G_{TS,X}$ and $G_{TS,Z}$ can be considered unity. In this case the output value of the tracking controllers can directly be used as compensation-based measurement result for the displacement of the target.

Post-print version of the article: E. Csencsics, "Integrated Compensation-based Laser Sensor System for In-plane and Out-of-plane Target Tracking," *Applied Optics*, vol. 59, no. 20, p. 6138-6147, 2020. DOI: 10.1364/AO.395572

5. Target Tracking Experiments

The performance of the compensation-based integrated laser sensor assembly is evaluated for single axis as well as combined dual axis motions by tracking the target which follows reference trajectories with a period of 120 s and a motion range of 1 mm. The frequency of the trajectories is chosen comparably small in order not to effect the tracking performance evaluation by the image processing delay. The outputs of the integrated laser sensor is fed back to the input of the tracking controllers, as shown in Fig. 8. For compensation-based determination of the relative position of the target (black) and the tracking platform (cyan), the setpoints of the target stages (d_x or d_z) and the output values of the tracking controllers (u_x or u_z) are used, respectively, as discussed in the previous section.

5.1. Tracking Motion in Single DoFs

For single axis motion the tracking controller of a single motion axis is switched on and a zero reference signal (r_x or r_z) is applied to the respective feedback, in order to maintain a constant lateral position or distance relative to the target. A sinusoidal reference signal (d_x or d_z) with a motion amplitude of 500 μm is applied to the respective target stage, resulting in a motion range of 1 mm. The target position (black) as well as the tracking stage position (cyan) is recorded by acquiring setpoint and controller output, respectively, and the resulting tracking error (red) is calculated accordingly.

The tracking result for in-plane displacements is depicted in Fig. 9a, showing that the tracking stage follows the target very well. The mean tracking error of 2.87 μm is below the resolution for in-plane motion and the standard deviation of 5 μm is still below pixel size. The peak-to-valley tracking error amounts to 28.1 μm, with a maximum error as small as 17.4 μm, equaling 1.74% of the entire motion range. Looking at the error distribution over the trajectory shape, the error during the steep trajectory slopes shows a comparably large uncertainty level, while around the turning points, where the slope is flatter, the uncertainty is significantly reduced and the offset becomes dominant. This can be explained by the tracking stage lagging behind the target stage due to the limited sensor resolution and the delayed action of the feedback controller, which first needs a tracking error in order to respond.

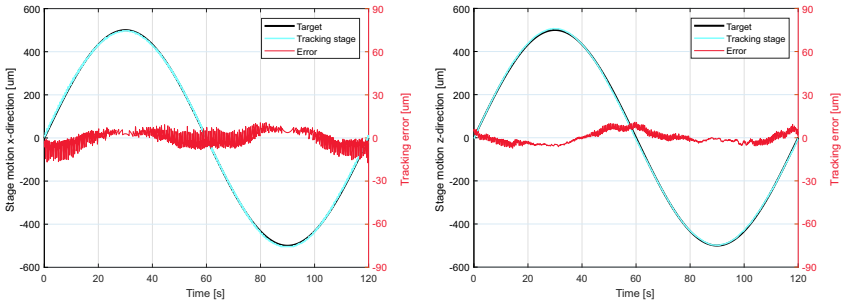

(a) In-plane (x-direction) displacement.

(b) Out-of-plane (z-direction) displacement.

Fig. 9. Compensation-based target tracking in single DoFs with enabled feedback control. (a) shows the system tracking in-plane motion of the target (x-axis). (b) depicts the system tracking out-of-plane motion of the target (z-axis).

The motions of the tracking stage and the target also show good agreement for out-of-plane displacements, as depicted in Fig. 9b. The remaining tracking error has a mean value of -0.45 μm,

Post-print version of the article: E. Csencsics, "Integrated Compensation-based Laser Sensor System for In-plane and Out-of-plane Target Tracking," *Applied Optics*, vol. 59, no. 20, p. 6138-6147, 2020. DOI: 10.1364/AO.395572

which is again below the resolution for out-of-plane displacements, and a standard deviation of 3.98 μm. The peak-to-valley tracking error amounts to 18.15 μm, with a maximum value as small as 10.9 μm, equaling 1.09% of the entire displacement. The tracking error has similar tendencies for the individual parts of the trajectory as for the in-plane motion but shows less uncertainty during the steep trajectory slopes, which can be explained by the higher resolution of the sensor for out-of-plane displacement.

5.2. *Combined Motion Tracking*

To evaluate the performance of the tracking system for simultaneous in-plane and out-of-plane displacements, a circular as well as a diamond shaped reference trajectory with amplitudes of 500 μm are used. For the circular trajectory two shifted sinusoidal signals are applied as reference signals to the target stages (d_x and d_z), while for the diamond trajectory two shifted triangular signals are used. The tracking controllers of both axes are enabled and again zero reference signals $r_x = r_z = 0$ are applied to the tracking feedback loops, to maintain a constant position relative to the target. Again the target position (black) as well as the tracking stage position (cyan) is recorded by acquiring the setpoints and controller outputs, respectively, and the resulting tracking error (red) is calculated accordingly.

The result for tracking the circular trajectory is depicted in Fig. 10a, showing good agreement of the target and tracking stage motions. The 2D trajectory starts at the point (red circle) indicated by $t = 0$ s and runs clockwise until reaching its starting point after 120 s. The spatial tracking error (green) is depicted around the origin, showing a maximum value of 21.45 μm and an rms value of 8.75 μm. The individual errors for in-plane and out-of-plane tracking are shown on the left and on the bottom of the trajectory plot, respectively. Indicating the trace and retrace error, the red line depicts the error of the trajectory part closer to the respective error graph, while the blue line depicts the error of the more distant trajectory part.

In x-direction there is a trailing error of the tracking stage observable, which is small in the beginning and around $t = 60$ s, due to the locally flat slopes in x-direction, and increases towards the steep slopes around $t = 30$ s and $t = 90$ s. This can again be explained by the tracking stage lagging behind the target stage due to the limited sensor resolution and the delayed action of the feedback controller, which first needs an error in order to respond. In z-direction the tracking error increases with negative sign in the beginning, again due to the steep slope in this region, and stays approximately constant around zero between x-values of 300 and -300 μm. It again increases around the steep slope of the trajectory around $t = 60$ s and becomes again constant thereafter. Compared to the x-axis, showing a gradually increasing trailing error, the tracking error of the z-axis increases solely around the outer positions, while remaining widely constant in between, which can be explained by the higher resolution of the z-axis. The offset of about 5 μm between the constant regions of trace and retrace error, as well as the small step after the second turnaround of the z-reference at $t = 90$ s may be explained by the mechanical play of one or both linear stages in this axis, which are specified with a bi-directional precision of ± 10 μm. As the tracking error in z-direction stays within the boundary of ± 26 μm, derived in Section 4.2, it can be concluded that the crosstalk to the x-direction stays below the sensor resolution.

In Fig. 10b the result for tracking the diamond trajectory is depicted, showing again good agreement of the stage motions with slight deviations around the turning points in z-direction. The spatial tracking error is again depicted around the origin (green), showing a maximum value of 37.33 μm and an rms value of 13.25 μm. The tendency of the tracking error in x-direction is comparable to the one of the circular trajectory, however, showing a larger level of uncertainty with a standard deviation of 8.24 μm, as compared to 5.16 μm for the circular trajectory. This can be explained by higher quantization errors of the sensor due to the constant steepness of the triangular trajectory. The error in z-direction is comparable for trace and retrace, is constantly increasing towards the turning point at $t = 30$ s and $t = 90$ s and decreasing towards the zero

Post-print version of the article: E. Csencsics, "Integrated Compensation-based Laser Sensor System for In-plane and Out-of-plane Target Tracking," *Applied Optics*, vol. 59, no. 20, p. 6138-6147, 2020. DOI: 10.1364/AO.395572

crossings of the triangular trajectory at t = 60 s and t = 120 s, respectively. Around the turning points in z-direction the tracking error shows a step with a height of about 8 μm. This may again be explained by the mechanical play of one or both of the linear z-stages, which was already observable for the circular trajectory, as well as by an overshoot of the tracking controller at the sharp turning points of the trajectory. The peak-to-valley error is with 29.25 μm about 50% larger than for the circular trajectory with 18.72 μm.

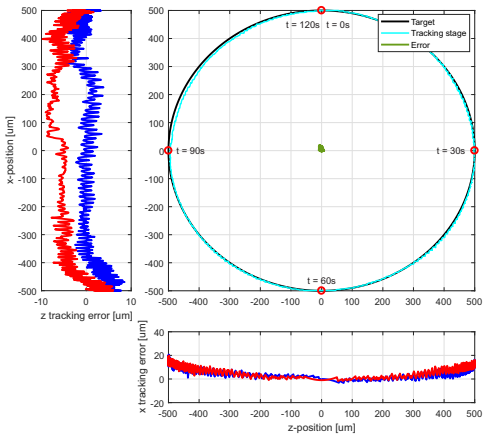

(a) Circular trajectory tracking.

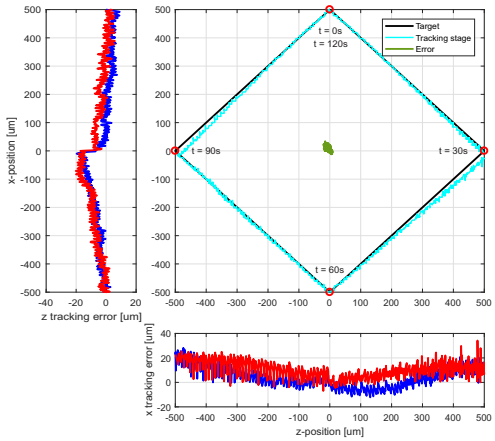

(b) Diamond shaped trajectory tracking.

Fig. 10. Simultaneous in-plane and out-of-plane target tracking. (a) shows the system tracking a circular trajectory. (b) depicts the system tracking a diamond shaped trajectory.

In summary it is successfully shown that the developed integrated sensor system in compensation-based operation has an in-plane and out-of-plane resolution of 3 μm and 1 μm and enables

Post-print version of the article: E. Csencsics, "Integrated Compensation-based Laser Sensor System for In-plane and Out-of-plane Target Tracking," *Applied Optics*, vol. 59, no. 20, p. 6138-6147, 2020. DOI: 10.1364/AO.395572

simultaneous accurate tracking of in-plane and out-of-plane displacements of a target with small tracking errors between 8.75 and 13.25 μm.

6. Conclusion

In this paper a compensation-based laser sensor, integrating laser triangulation and OLSP measurements principles, is developed for a tracking system able to follow the in-plane and out-of-plane motions of a target with optically rough surface. The sensor design is based on a modified OLSP assembly, extended by an aperture which reduces the effectively illuminated detector area but still enables the formation of objective speckles to measure in-plane displacement. By additionally evaluating the center of gravity of the illuminated area, which changes with distance to the target and resembles the triangulation principle, also the sensing of out-of-plane displacement is enabled. The tradeoff between aperture distance and sensitivity is investigated and the crosstalk between the DoFs is found to be negligible for the compensation-based use of the designed sensor. The resulting sensor has an in-plane and out-of-plane resolution of 3 μm and 1 μm, respectively, a sample rate of about 10 Hz and, due to the compensation-based operation, a large operation range, only limited by the range of the positioning system. With the designed tracking control structure, centered around two integral controllers, the laser sensor is turned into a zero detector for both DoFs and the tracking system performance is evaluated for sinusoidal (1D), circular and diamond shaped (2D) motion trajectories. It is demonstrated that with the integrated laser sensor the tracking system can accurately follow the 2D trajectories in an area of 1 x 1 mm with a small spatial rms error between 8.75 and 13.25 μm.

As the prototype implements the OLSP configuration with sensitivity to crosstalk from out-of-plane motions, it is reasonable to assume that the second in-plane DoF, showing no sensitivity to out-of-plane crosstalk, can immediately be used to extend the tracking capabilities of the sensor to all 3 translational DoFs. The range of the developed compensation-based laser sensor system is eventually only limited by the range of the tracking actuation system, while providing the full resolution over the entire motion range. For real-world applications it is to be pointed out that the measurement rate of the sensor will need significant improvement in order to limit motion blurring effects in the speckle pattern due to higher target speeds. To enable the capturing of typical vibrations in industrial environments with significant amplitudes and frequency components of several hundred Hertz also calls for a faster sensor, as the sampling rate has to be at least twice the maximum vibration component in an actual application. Thus, future work will be concerned with integrating the sensor design into a compact sensor head as well as with increasing the computational efficiency and therewith the resolution and bandwidth of the sensor.

Acknowledgments

The author would like to thank Tobias Wolf for his support with the construction and evaluation of the prototype system as well as for his assistance with the conducted measurements.

Disclosures

The authors declare no conflicts of interest.

References

1. M. Thier, R. Saathof, A. Sinn, R. Hainisch, and G. Schitter, "Six degree of freedom vibration isolation platform for in-line nano-metrology," IFAC-PapersOnLine **49**, 149–156 (2016).
2. Y. Chen and F. Dong, "Robot machining: recent development and future research issues," The Int. J. Adv. Manuf. Technol. **66**, 1489–1497 (2013).
3. M. Ries, B. D. D. Senneville, S. Roujol, Y. Berber, B. Quesson, and C. Moonen, "Real-time 3d target tracking in mri guided focused ultrasound ablations in moving tissues," Magn. Reson. Medicine **64**, 1704–1712 (2010).

4. A. Krupa, G. Fichtinger, and G. D. Hager, "Full motion tracking in ultrasound using image speckle informationand visual servoing," Proc. 2007 IEEE Int. Conf. on Robotics Autom. pp. 2458–2464 (2007).
5. D. Imkamp, R. Schmitt, and J. Berthold, "Blick in die zukunft der fertigungsmesstechnik - die vdi/vde-gma roadmap fertigungsmesstechnik 2020," Tech. Messen **10**, 433–439 (2012).
6. D. Wertjanz, E. Csencsics, J. Schlarp, and G. Schitter, "Design and control of a maglev platform for positioning in arbitrary orientations," IEEE Adv. Intell. Mechatronics Conf. Boston, USA, print (2020).
7. J. Schlarp, E. Csencsics, and G. Schitter, "Optical scanning of a laser triangulation sensor for 3d imaging," IEEE Transactions on Instrumentation Meas. print (2020).
8. C. P. Keferstein and W. Dutschke, *Fertigungsmesstechnik* (Springer Vieweg, Wiesbaden, 2010).
9. F. J. Brosed, J. J. Aguilar, D. Guilloma, and J. Santolaria, "3d geometrical inspection of complex geometry parts using a novel laser triangulation sensor and a robot," Sensors **11**, 90–110 (2010).
10. M. A. Sutton, J. J. Orteu, and H. Schreier, *Image correlation for shape, motion and deformation measurements: basic concepts, theory and applications* (Springer Science & Business Media, New York, USA, 2009).
11. P. K. Rastogi and D. Inaudi, *Optical Non-Destructive Testing and Inspection* (Elsevier Science, Ltd., Oxford, UK, 2000).
12. P. K. Rastogi, *Digital Speckle Pattern Interferometry and Related Techniques* (John Wiley & Sons Ltd, Chichester, England, 2000).
13. I. Yamaguchi, "Speckle displacement and decorrelation in the diffraction and image fields for small object deformation," Opt. Acta: Int. J. Opt. **28**, 1359–1376 (1981).
14. R. Paris, T. Thurner, and G. Schitter, "Compensation based displacement measurement using objective laser speckles," IFAC Proc. Vol. **46**, 264–270 (2013).
15. S. Schneider, Y. Gautam, and B. Zagar, "Application of a locally operating laser-speckle strain sensor," IEEE Transactions on Instrumentation Meas. **52**, 1025–1029 (2003).
16. I. Yamaguchi, T. Takemori, and K. Kobayashi, "Stabilized and accelerated speckle strain gauge," Opt. engineering **32**, 618–625 (1993).
17. T. O. Charrett, Y. K. Bandari, F. Michel, J. Ding, S. W. Williams, and R. P. Tatam, "A non-contact laser speckle sensor for the measurement of robotic tool speed," Robotics Comput. Manuf. **53**, 187–196 (2018).
18. T. O. H. Charrett, T. Kissinger, and R. P. Tatam, "Workpiece positioning sensor (wpos): A three-degree-of-freedom relative end-effector positioning sensor for robotic manufacturing," Procedia CIRP **79**, 620–625 (2019).
19. R. Paris, M. Melik-Merkumians, and G. Schitter, "Probabilistic absolute position sensor based on objective laser speckles," IEEE Transactions on Instrumentation Meas. **65**, 1188–1196 (2016).
20. G. Schitter, A. Stemmer, and F. Allgoewer, "Robust two-degree-of-freedom control of an atomic force microscope," Asian J. Control. **6**, 156–163 (2004).
21. A. Donges and R. Noll, *Laser measurement technology* (Springer-Verlag Berlin AN, 2016).
22. H. Khali, Y. Savaria, J.-L. Houle, M. Rioux, J.-A. Beraldin, and D. Poussart, "Improvement of sensor accuracy in the case of a variable surface reflectance gradient for active laser range finders," IEEE Transactions on Instrumentation Meas. **52**, 1799–1808 (2003).
23. S. Werling, M. Mai, M. Heizmann, and J. Beyerer, "Inspection of specular and partially specular surfaces," Metrol. Meas. Syst. **16**, 415–431 (2009).
24. F. Blais, M. Rioux, and J.-A. Beraldin, "Practical considerations for a design of a high precision 3-d laser scanner system," Optomech. electro-optical design industrial systems **959**, 225–246 (1988).
25. L. Shen, D. Li, and F. Luo, "A study on laser speckle correlation method applied in triangulation displacement measurement." Optik **124**, 4544–4548 (2013).
26. J. W. Goodman, "Some fundamental properties of speckle," J. Opt. Soc. Am. **66**, 1145–1150 (1976).
27. P. Rastogi and D. Inaudi, eds., *Trends in Optical Non-Destructive Testing* (Elsevier Science, Kidlington, Oxford, England, 2000).
28. M. Sjoedahl, "Calculation of speckle displacement, decorrelation, and object-point location in imaging systems," Appl. Opt. **34**, 7998–8010 (1995).
29. M. Sjoedahl, "Accuracy in electronic speckle photography," Appl. Opt. **36**, 2875–2885 (1997).
30. J. W. Goodman, *Statistical optics* (Wiley-Interscience New York, 1985).

Post-print version of the article: E. Csencsics, "Integrated Compensation-based Laser Sensor System for In-plane and Out-of-plane Target Tracking," *Applied Optics*, vol. 59, no. 20, p. 6138-6147, 2020. DOI: 10.1364/AO.395572